

# Uracil Adsorbed on Si(001): Structure and Energetics

K. Seino,<sup>†</sup> W. G. Schmidt,\* M. Preuss, and F. Bechstedt

*Institut für Festkörpertheorie und Theoretische Optik, Friedrich-Schiller-Universität Jena, Max-Wien-Platz 1, 07743 Jena, Germany*

*Received: January 30, 2003; In Final Form: March 30, 2003*

The adsorption of uracil on the Si(001) surface has been investigated by density-functional theory calculations using a plane-wave basis in conjunction with ultrasoft pseudopotentials. A large number of possible interface structures are studied. Electrostatic effects and the keto–enol tautomerism play an important role for the surface reaction. There exists a pronounced tendency for molecular fragmentation, leading to the dissociation of hydrogen from the molecules and possibly to oxygen insertion into Si dimers.

## 1. Introduction

The chemistry of small organic and biological molecules on Si(001) surfaces is of both fundamental and technological interest.<sup>1–3</sup> This interest arises from the vast range of qualities that organic molecules can be designed to have and the hope of adding their functionality to semiconductor technology. A detailed understanding of the adsorbate–surface structure is required in order to control the incorporation of the functionality. Much progress has been made in recent years in understanding the reaction of simple unsaturated organic molecules with the Si(001) surface. Previous studies showed that alkenes can react with Si dimers via a [2 + 2] cycloaddition reaction and may thus form very well ordered organic films.<sup>4–6</sup> Potentially more interesting are surface reactions with polyfunctional organic molecules. They may allow for creating an ordered array of possible further reaction sites, provided the functional groups remain intact. However, the interaction of polyfunctional organic molecules with semiconductor surfaces is often poorly understood, because of the many surface reactions possible. Molecules containing two conjugated double bonds may react with the Si(001) surface via [4 + 2] Diels–Alder reactions<sup>3</sup> as well as via [2 + 2] cycloadditions. A large variety of interface structures may form for heterocyclic amines, which in addition to C=C double bonds also contain N–H bonds. The configuration formed via N–H bond cleavage is favorable in the case of pyrrole; for example, see refs 7–10. [2 + 2] C=O cycloaddition reactions as well as  $\alpha$ -hydrogen transfers to Si dangling bonds are discussed for the adsorption of ketones on Si(001).<sup>11–14</sup>

In the present study we investigate as a model case the chemisorption of uracil on the Si(001) surface. This system was previously investigated with scanning tunneling microscopy (STM) and high-resolution electron energy-loss spectroscopy (HREELS).<sup>15</sup> The STM images show that uracil may form ordered overlayer structures. The HREELS spectra yield a stronger intensity of the in-plane modes compared with the out-of-plane vibrations, indicating that the orientation of the molecular plane is upright. Some uracil/Si(001) bonding configurations were also already probed computationally, using an eight-atom cluster to model the Si surface.<sup>15</sup> Uracil contains one C=C double bond, two N–H bonds, and two carbonyl

bonds (C=O). Therefore, surface reaction scenarios similar to the ones discussed above for alkenes, amines, or ketones may occur and are investigated in the present study using *first-principles* calculations.

## 2. Computational Method

The total-energy and electronic-structure calculations are performed using the Vienna ab initio simulation package (VASP) implementation<sup>16</sup> of the gradient-corrected<sup>17</sup> density functional theory (DFT-GGA). The electron–ion interaction is described by non-normconserving ultrasoft pseudopotentials,<sup>18,19</sup> allowing for the accurate quantum-mechanical treatment of first-row elements with a relatively small basis set of plane waves. We expand the electronic wave functions into plane waves up to an energy cutoff of 25 Ry, which has been demonstrated to be sufficient in our previous studies on pyrrole adsorption<sup>10</sup> and DNA base molecules.<sup>20</sup>

The Si(001) surface is modeled with a periodically repeated slab. The supercell consists of 8 atomic Si layers plus adsorbed molecules and a vacuum region equivalent in thickness to 12 atomic layers. The Si bottom layer is hydrogen saturated and kept frozen during the structure optimization. All calculations are performed using the calculated Si equilibrium lattice constant of 5.456 Å. Depending on the molecule coverage investigated, supercells with (4 × 2), (4 × 1), (2 × 2), or (2 × 1) surface periodicity are used. The topmost 5 layers of the slab as well as the adsorbed molecules are allowed to relax. Calculations for gas-phase molecules were performed using 12 × 12 × 10 Å<sup>3</sup> supercells.

The residual minimization method—direct inversion in the iterative subspace (RMM-DIIS) algorithm<sup>16,21,22</sup> is employed to minimize the total energy of the system. The surface structure is considered to be in equilibrium when the Hellmann–Feynman forces are smaller than 10 meV/Å. The Brillouin zone integrations are performed using sets corresponding to 64k points in the full (1 × 1) surface Brillouin zone.

## 3. Results and Discussion

Uracil exists in several tautomeric forms. Twelve forms, except uracil itself (U<sub>1</sub> in Figure 1), may form. The diketo form (U<sub>1</sub>) is energetically most favored (see, e.g., ref 23). To explain the absence of C=O bond-related vibrations, Lopez and co-workers<sup>15</sup> suggested that the uracil/Si(001) interface formation

\* To whom correspondence should be addressed. E-mail: wgs@ifto.physik.uni-jena.de.

<sup>†</sup> E-mail: seino@ifto.physik.uni-jena.de.

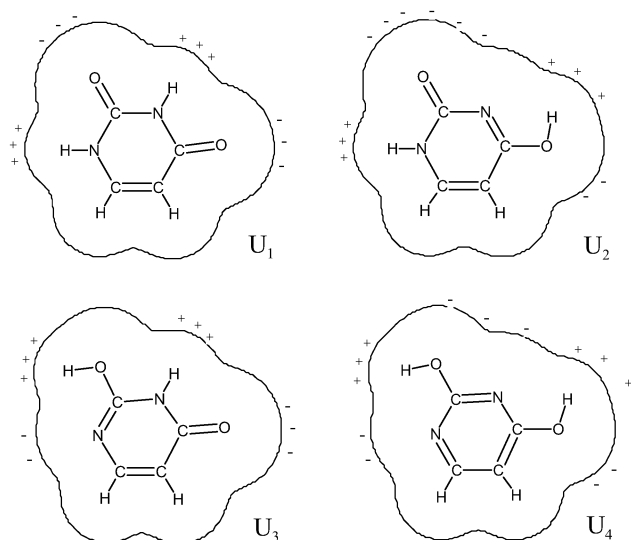


**Figure 1.** Tautomeric forms of uracil. The contour lines represent a charge density of  $\rho = 0.005 \text{ e}/\text{\AA}^3$ . The calculated electrostatic potential around the molecules is indicated.

**TABLE 1: Relative Energies  $E_{\text{diff}}$  in eV of Tautomer Molecules Calculated Here (DFT-GGA) and in Ref 23 (B3LYP/6-31+G(dp))**

	U <sub>1</sub>	U <sub>2</sub>	U <sub>3</sub>	U <sub>4</sub>
$E_{\text{diff}}^{\text{DFT-GGA}}$	0	0.51	0.53	0.64
$E_{\text{diff}}^{\text{B3LYP}}$	0	0.51	0.48	0.55

involves the enol tautomer. The calculated relative formation energies in the gas-phase for the most stable 2,4-dienol tautomer (U<sub>4</sub> in Figure 1) as well as the most favored keto–enol tautomers with one hydroxyl group and one carbonyl group (U<sub>2</sub> and U<sub>3</sub>) are compiled in Table 1. In agreement with previous studies,<sup>23</sup> we find the dienol tautomer energetically to be the least favored, and the energy difference between the 2-oxo-4-hydroxy tautomer (U<sub>2</sub>) and the 2-hydroxy-4-oxo tautomer (U<sub>3</sub>) to be small. The relative order of U<sub>2</sub> and U<sub>3</sub>, however, is reversed in comparison to the results of ref 23. The energy difference between these two structures is of the order of the error bar of our total-energy calculations.

On the basis of the calculated results for the gas-phase molecules discussed above, we concentrate at first on the adsorption of the diketone tautomer on the Si(001) surface. The [2 + 2] cycloaddition reaction (Figure 2a) results for 0.25 monolayer (ML) in an energy gain of 0.75 eV (cf. Table 2).

**TABLE 2: Calculated Uracil Adsorption Energies in eV/molecule for Different Coverages with Respect to the  $c(4 \times 2)$  Reconstructed Surface Ground State of Si(001)<sup>a</sup>**

geometry	adsorption energy		
	0.25 ML	0.5 ML	1 ML
a	0.75		0.89
b	0.63		1.02
c	1.59	1.56	1.49
d	1.76		1.49
e	2.77	2.44	
f	0.48		
g	0.99		
h	1.15		
i	1.77		
j	3.66	3.84	
k	3.78		
l	4.63		
m	5.27		
n	2.71		

<sup>a</sup> The labeling of the geometries refers to Figure 2.

There are several possible molecular arrangements for the full monolayer coverage. We find it most favorable when the mirror symmetry is broken, that is, when molecules adsorbed on adjacent Si dimers are rotated by 180° with respect to each other. The attractive interaction between the molecules increases the adsorption energy to 0.89 eV. Compared to previous calculations for the [2 + 2] cycloaddition of cyclopentene on Si(001), the value for the adsorption energy presented here is of the same order<sup>24</sup> or slightly lower.<sup>25,26</sup> The adsorption energy calculated in ref 14 for the [2 + 2] cycloaddition of simple unsaturated ketones on Si(001), on the other hand, is more than twice the value predicted here. That difference may be related to the fact that the Si surface in ref 14 was modeled by a nine-atom cluster (cf. also discussion in ref 27).

In a series of recent studies on the adsorption of acetylene on Si(001),<sup>28–32</sup> a so-called end-bridge configuration was found to lead to a similar adsorption energy to that of the [2 + 2] cycloaddition. In this configuration the molecule bridges the ends of two adjacent dimers in a Si dimer row (cf. Figure 2b). In the case of uracil, the adsorption energy is slightly lower than the corresponding cycloaddition value for quarter monolayer coverage. On the other hand, increasing the coverage to 1 ML renders the end-bridge configuration more favorable than the cycloaddition. This tendency agrees with the findings for acetylene on Si(001).<sup>29–31</sup> Again, for electrostatic reasons, a configuration where every second molecule is rotated by 180° is energetically favored.

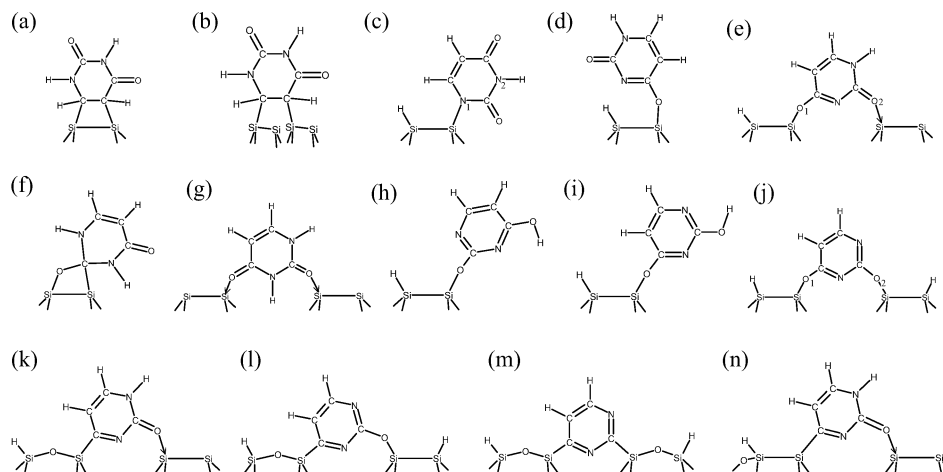


**Figure 2.** Schematic illustrations of possible uracil/Si(001) interface structures. Arrows represent dative bonds.

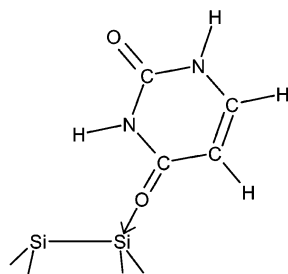


**Figure 3.** Schematic illustration of the dative-bond state for the uracil adsorption on the Si(001) surface.

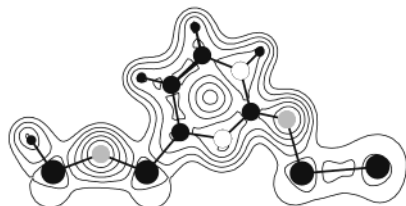


**Figure 4.** Calculated valence charge density for the structure in Figure 2e. The contours are logarithmically spaced from  $2^{-2}$  to  $2^2 e/\text{\AA}^3$ . Large, medium, and small black circles represent Si, C, and H atoms, respectively. Gray and white circles represent O and N atoms, respectively.

We investigated a series of N–H dissociative adsorptions with different nitrogen atoms involved ( $N_1$  or  $N_2$ ) and different molecular arrangements. All of these structures give rise to an adsorption energy in the range 1.3–1.6 eV, larger than that released upon cycloaddition or the formation of the end-bridge structure. The most favorable N–H dissociative model found in our study is shown in Figure 2c.

On the basis of previous investigations studying ketones adsorbed on Si(001),<sup>11–14</sup> also reactions of the carbonyl group are considered. The respective adsorption energies for the formation of enol-like interface structures (cf. Figure 2d and e) and a  $[2 + 2]$  C=O cycloaddition (Figure 2f) are given in Table 2. A likely precursor state for these interface structures may be a dative-bonded configuration, as shown in Figure 3.<sup>13,14</sup> In this state the molecules donate charge from the lone pair of the O atom into the empty Si surface dangling bond. We calculate an adsorption energy of 0.39 eV for this configuration. The most favorable bonding configuration of the class of carbonyl-group related reactions is given by the structure shown in Figure 2e. The  $O_1$ –Si/ $O_2$ –Si bond lengths amount to 1.74/1.85 Å. While the second bond is weaker and slightly larger than the sum of the oxygen and silicon covalent radii, that is, of dative-bond character, the accumulation of bond charge is comparable to the one for the  $O_1$ –Si bond, as can be seen from the charge density plot in Figure 4. The stability of the structure in Figure 2e can be understood on the basis of electrostatic interactions: Clean Si(001) surfaces reconstruct due to the dimerization of the topmost atoms. The dimers are asymmetric, consisting of an  $sp^2$ -like bonded “down” atom, which moves closer to the plane of its three nearest neighbors, and an “up” atom, which moves away from the plane of its neighbors and possesses an s-like dangling bond. The process of rehybridization is accompanied by a charge transfer from the “down” to the “up” atom. The direction of buckling alternates within each dimer row. To reduce the energy due to relaxation of local stress and electrostatics, the buckling in the neighboring dimer rows is such that the Si(001) surface ground state is  $c(4 \times 2)$  reconstructed.<sup>33,34</sup> Therefore, two “electron-poor” Si dimer atoms are situated next to each other across the Si dimer rows. This configuration favors the attachment of the “electron-rich”

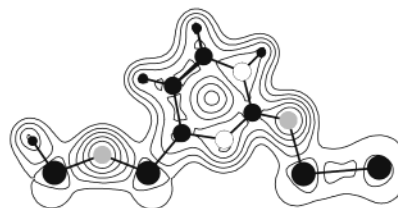


**Figure 5.** Calculated valence charge density for the structure in Figure 2k. The contours are logarithmically spaced from  $2^{-2}$  to  $2^2 e/\text{\AA}^3$ . Large, medium, and small black circles represent Si, C, and H atoms, respectively. Gray and white circles represent O and N atoms, respectively.

carbonyl groups of uracil in such a way that the dimer rows are bridged. However, electrostatics alone is not sufficient to explain the uracil adsorption. This becomes obvious from the relatively low adsorption energy of the double dative-bonded state shown in Figure 2g.

The study by Lopez et al.<sup>15</sup> suggests that the adsorption involves enol or keto–enol tautomers (cf. Figure 1) of uracil. Therefore, dissociations of the hydroxyl groups (–OH) are investigated, similar to the cases of methanol<sup>35,36</sup> and ethanol<sup>37</sup> adsorption on Si(001). For this class of reactions we consider the two cases shown in Figure 2h and i. These two models are proposed on the basis of HREELS data, indicating the absence of C=O bonds at the surface.<sup>15</sup> We find the energy difference between these two models to be much larger than that in previous quantum chemistry calculations<sup>15</sup> (cf. Table 2). This may be related to the molecular interaction with neighboring Si dimers, which were not included in the cluster calculations. Nevertheless, compared to the case of structure e in Figure 2, which was not considered previously, the adsorption of the dienol tautomer of uracil in structures h and i is energetically not favored. The adsorption of the enol tautomer, however, is favorable if two Si dimers are involved in the reaction, as shown in Figure 2j. This structure may be formed either by dienol tautomer adsorption or by  $\alpha$ -hydrogen transfer. The adsorption energy of structure j is 3.66 eV, about 1 eV more than that for configuration e. The higher adsorption energy is due to stronger molecule–surface bonds: the  $O_1$ –Si and  $O_2$ –Si bond lengths are about 1.7 Å, much shorter than those for model e. Increasing the coverage from 0.25 to 0.5 ML leads to a further increase in the adsorption energy, from 3.66 to 3.84 eV.

The Si dimer bond is the target for the initial insertion of oxygen into the Si(001) surface, following water exposure and annealing.<sup>38</sup> Oxygen insertion is also discussed in the case of ketones adsorbed on Si(001).<sup>13</sup> Cycloaddition products formed by organic molecules with carbonyl groups on Si(001) can rearrange to lower their energy by oxygen migration.<sup>12</sup> Prompted by these findings, we investigate the insertion of oxygen into Si–Si bonds. The structures shown in Figure 2e and j may be possible starting points for the insertion of one or two oxygen atoms into the Si surface dimers. As can be seen from Table 2, the formation of Si–O–Si bonds in the uppermost Si surface layer is energetically very favorable (cf. structures k, l, and m in Figure 2). The formation of strong covalent Si–O bonds can be seen from the charge density plot in Figure 5. In contrast, the oxygen incorporation into the Si back-bonds is less favorable, at least for the configuration studied here, shown in Figure 2n. This may indicate that uracil adsorption prevents subsequent oxidation of the Si layers beneath the surface.

Together with the oxygen insertion structures discussed above, the models shown in Figure 2e and j are the energetically most favored configurations. In addition, these models are consistent

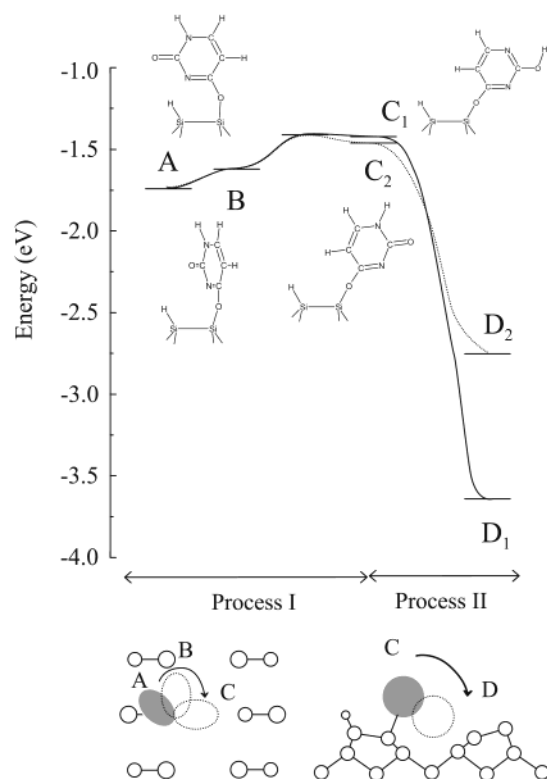


**Figure 6.** Calculated reaction barriers for the transition from structure d in Figure 2 to models e and j shown in Figure 2. A, D<sub>2</sub>, and D<sub>1</sub> correspond to models d, e, and j, respectively.

with experiment:<sup>15</sup> Lopez et al. concluded that Si—H and Si—O but no C=O bonds are present at the surface. However, to establish whether these structures will indeed form, total-energy calculations are not sufficient. In addition, the calculation of the reaction barriers is needed.

Previous calculations for ketones attached to the Si(001) surface<sup>13,14</sup> showed that the energy barrier for the transition from the dative-bonded state shown in Figure 3 to an enol-like product such as that shown in Figure 2d (labeled A in Figure 6) is small, of the order of 0.1–0.2 eV. Therefore, we take structure A in Figure 6 as the starting point for the calculation of the reaction paths toward the energetically favored structures e and j shown in Figure 2 (corresponding to D<sub>2</sub> and D<sub>1</sub> in Figure 6). In detail, we consider two steps: A rotation around the surface normal (process I in Figure 6) and the tilting toward the neighboring Si dimer (process II in Figure 6). To form the structure D<sub>1</sub>, in addition a diketo to keto–enol transition is needed (C<sub>2</sub> vs C<sub>1</sub> in Figure 6). This requires no additional energy barrier, showing that the formation of the keto–enol tautomer is more favorable for the adsorbed molecule than for gas-phase uracil (cf. Table 1). In both cases, the energy barrier amounts to 0.33 eV for the rotation. There is no barrier for the tilting of the molecule into the dimer-row bridging position. Our results thus indicate that both interface structures shown in Figure 2e and j may easily form at room temperature.

The energy barrier for the N–H dissociative adsorption shown in Figure 2c is small, of the order of one tenth of an electronvolt, as can be concluded from previous calculations for the pyrrole/Si(001) interface.<sup>10</sup> The transition from structure c in Figure 2 to the energetically more favored surface geometries e and j requires substantial structural and chemical interface modifications. Therefore, one could suspect that a significant amount of uracil is bonded to the surface according to the scheme in Figure 2c. However, moderate annealing to 313 K results in a

significant loss of intensity of the N–H stretching and carbonyl HREELS bands.<sup>15</sup> This indicates a transitory character for structure c.

Using the nudged elastic band method,<sup>39</sup> we also calculated the energy barrier for the oxygen insertion into the Si dimers. The formation of the oxidized structure shown in Figure 2k requires that a relatively large energy barrier of more than 1.2 eV be overcome.

In conjunction with the experimental findings,<sup>15</sup> our results thus indicate that for moderate annealing temperatures the uracil/Si(001) interface is characterized by the structures shown in Figure 2e and j, with the dimer bridging configuration (j) dominating. The attractive interaction between the uracil molecules adsorbed in configuration j may explain the preference of the uracil molecules to form ordered lines parallel to the dimer rows, as seen with STM.<sup>15</sup>

#### 4. Summary

Several plausible interface configurations for uracil adsorbed on Si(001) have been calculated from *first-principles*. Among the structures investigated, we find that oxygen insertion into Si surface dimers is energetically most favored. It requires, however, that a considerable energy barrier be overcome. For moderate annealing temperatures, our calculations predict the formation of a structure where uracil bridges two neighboring Si-dimer rows. The energetically favored structures are in accord with the available experimental data.

**Acknowledgment.** Grants of computer time from the Leibniz-Rechenzentrum München, the Höchstleistungs-Rechenzentrum Stuttgart, and the John von Neumann-Institut Jülich are gratefully acknowledged.

#### References and Notes

- (1) Wolkow, R. A. *Annu. Rev. Phys. Chem.* **1999**, *50*, 413.
- (2) Hamers, R. J.; Coulter, S. K.; Ellison, M. D.; Hovis, J. S.; Padowitz, D. F.; Schwartz, M. P.; Greenleaf, C. M.; Russell, J. N., Jr. *Acc. Chem. Res.* **2000**, *33*, 617.
- (3) Bent, S. F. *J. Phys. Chem. B* **2002**, *106*, 2830.
- (4) Hamers, R. J.; Hovis, J. S.; Lee, S.; Liu, H.; Shan, J. *J. Phys. Chem. B* **1997**, *101*, 1489.
- (5) Hovis, J. S.; Lee, S.; Liu, H.; Hamers, R. J. *J. Vac. Sci. Technol., B* **1997**, *15*, 1153.
- (6) Hovis, J. S.; Liu, H.; Hamers, R. J. *Appl. Phys. A* **1998**, *66*, S553.
- (7) Qiao, M. H.; Cao, Y.; Deng, J. F.; Xu, G. Q. *Chem. Phys. Lett.* **2000**, *325*, 508.
- (8) Cao, X.; Coulter, S. K.; Ellison, M. D.; Liu, H.; Liu, J.; Hamers, R. J. *J. Phys. Chem. B* **2001**, *105*, 3759.
- (9) Luo, H.; Lin, M. C. *Chem. Phys. Lett.* **2001**, *343*, 219.
- (10) Seino, K.; Schmidt, W. G.; Furthmüller, J.; Bechstedt, F. *Phys. Rev. B* **2002**, *66*, 235323.
- (11) Armstrong, J. L.; White, J. M.; Langell, M. J. *Vac. Sci. Technol., A* **1997**, *15*, 1146.
- (12) Barriocanal, J. A.; Doren, D. J. *J. Am. Chem. Soc.* **2001**, *123*, 7340.
- (13) Wang, G. T.; Mui, C.; Musgrave, C. B.; Bent, S. F. *J. Phys. Chem. B* **2001**, *105*, 12559.
- (14) Wang, G. T.; Mui, C.; Musgrave, C. B.; Bent, S. F. *J. Am. Chem. Soc.* **2002**, *124*, 8990.
- (15) Lopez, A.; Chen, Q.; Richardson, N. V. *Surf. Interface Anal.* **2002**, *33*, 441.
- (16) Kresse, G.; Furthmüller, J. *Comput. Mater. Sci.* **1996**, *6*, 15.
- (17) Perdew, J. P.; Chevary, J. A.; Vosko, S. H.; Jackson, K. A.; Pederson, M. R.; Singh, D. J.; Fiolhais, C. *Phys. Rev. B* **1992**, *46*, 6671.
- (18) Vanderbilt, D. *Phys. Rev. B* **1990**, *41*, 7892.
- (19) Furthmüller, J.; Käckell, P.; Bechstedt, F.; Kresse, G. *Phys. Rev. B* **2000**, *61*, 4576.
- (20) Preuß, M.; Schmidt, W. G.; Seino, K.; Furthmüller, J.; Bechstedt, F. *J. Comput. Chem.*, submitted.
- (21) Pulay, P. *Chem. Phys. Lett.* **1980**, *73*, 393.
- (22) Wood, D. M.; Zunger, A. *J. Phys. A* **1985**, *18*, 1343.
- (23) Kryachko, E. S.; Nguyen, M. T.; Zeegers-Huyskens, T. *J. Phys. Chem. A* **2001**, *105*, 1288.



- (24) Lu, W.; Schmidt, W. G.; Bernholc, J. *Phys. Rev. B*, submitted.
- (25) Cho, J.-H.; Kleinman, L. *Phys. Rev. B* **2001**, *64*, 235420.
- (26) Akagi, K.; Tsuneyuki, S. *Surf. Sci.* **2001**, *493*, 131.
- (27) Penev, E.; Kratzer, P.; Scheffler, M. *J. Chem. Phys.* **1999**, *110*, 3986.
- (28) Sorescu, D. C.; Jordan, K. D. *J. Phys. Chem. B* **2000**, *104*, 8259.
- (29) Morikawa, Y. *Phys. Rev. B* **2001**, *63*, 033405.
- (30) Kim, W.; Kim, H.; Lee, G.; Hong, Y.-K.; Lee, K.; Hwang, C.; Kim, D.-H.; Koo, J.-Y. *Phys. Rev. B* **2001**, *64*, 193313.
- (31) Miotto, R.; Ferraz, A. C.; Srivastava, G. P. *Phys. Rev. B* **2002**, *65*, 075401.
- (32) Wang, F.; Sorescu, D. C.; Jordan, K. D. *J. Phys. Chem. B* **2002**, *106*, 1316.
- (33) Dabrowski, J.; Müssig, H.-J. *Silicon Surfaces and Formation of Interfaces*; World Scientific: Singapore, 2000.
- (34) Krüger, P.; Pollmann, J. *Phys. Rev. Lett.* **1995**, *74*, 1155.
- (35) Kato, T.; Kang, S.-Y.; Xu, X.; Yamabe, T. *J. Phys. Chem. B* **2001**, *105*, 10340.
- (36) Casaletto, M. P.; Zanoni, R.; Carbone, M.; Piancastelli, M. N.; Aballe, L.; Weiss, K.; Horn, K. *Surf. Sci.* **2002**, *505*, 251.
- (37) Casaletto, M. P.; Zanoni, R.; Carbone, M.; Piancastelli, M. N.; Aballe, L.; Weiss, K.; Horn, K. *Surf. Sci.* **2000**, *447*, 237.
- (38) Weldon, M. K.; Stefanov, B. B.; Raghavachari, K.; Chabal, Y. J. *Phys. Rev. Lett.* **1997**, *79*, 2851.
- (39) Mills, G.; Jonsson, H.; Schenter, G. K. *Surf. Sci.* **1995**, *324*, 305.